

# Visual Analysis of Zebrafish Behavior

Tobias Palmér      Kalle Åström  
Centre of Mathematical Sciences  
Lund University  
{tobiasp,kalle}@maths.lth.se

Olof Enqvist  
Dep. of Signals and Systems  
Chalmers University of Technology  
olof.enqvist@chalmers.se

Per Petersson  
Dep. of Experimental Medical Sciences, NRC  
Lund University  
per.petersson@med.lu.se

**Abstract**—There is significant interest from the medical and neuroscience communities for studying the behavior of zebrafish larvae, particularly in the context of drug testing. In this paper, we propose a method for analyzing the behavior of zebrafish larvae in a high-throughput system using automatic image analysis. Specifically, algorithms for estimating the poses of the larvae in video recordings are presented. The pose estimation results are subsequently used to estimate kinematic parameters, segment the discretized movement into swim bouts (short bursts of movement) and to categorize the swim bouts into a number of classes. The distributions of bout classes are analyzed over time for different doses of amphetamine and apomorphine and compared to control groups. Preliminary results are presented indicating that the proposed method is able to measure the effects of pharmacological manipulations in the zebrafish larvae.

## I. INTRODUCTION

Automatic image analysis for the purpose of analyzing the behavior of animals is a commonly used tool in for example medicine and biology [1]–[10]. When used appropriately, it has the potential of greatly improving upon the quantity and/or quality of data gathering.

Zebrafish is a popular model animal in the field of medicine, but up until recently the commercially available automatic tracking softwares have tracked only one position per fish, consequently greatly limiting the behavioral analysis. However, some papers present more advanced whole-body tracking and analysis of curvature and bending motion of the fish. Fontaine et al. proposes a method for tracking zebrafish using a geometrical model of the fish [11], applied on videos recorded at 1500 fps with  $1024 \times 1024$  pixels resolution. Tian et al. presents a method for tracking a single zebrafish in two cameras recording up to 250 fps at  $640 \times 480$  pixels resolution [5].

Here, however, we choose a compromise between quantity and quality of tracking. A high-throughput system for automatic tracking and analysis of zebrafish larvae behavior is presented, using a skeleton-based model of the larvae. A single camera recording 300 fps at  $640 \times 480$  pixels resolution is used for recording the behavior of 48 spatially separated larvae. The high frame rate enables the detection of quick movements and a higher temporal consistency than lower frame rates would, while the large number of animals makes the system practically useful for evaluating the effects of various stimuli.

## II. EQUIPMENT AND VIDEO DATA

The behavioral setup consisted of a 300 fps digital camera with a resolution of  $640 \times 480$  pixels (Genie HM640, Teledyne DALSA, Waterloo, Canada) connected to a computer with

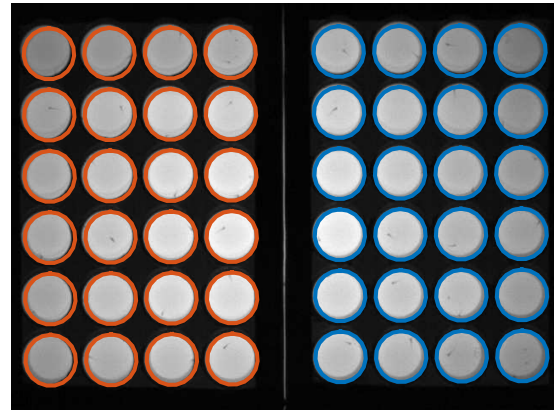


Fig. 1. An image from the video where zebrafish larvae have been placed in two 24 well microtiter plates. Superimposed projections of the geometric model of the microtiter plates are plotted in red and blue.

video recording software (CamExpert v7.00.00.0912, Teledyne DALSA, Waterloo, Canada; LabVIEW 2011 v11.0, National Instruments, Austin, TX). In each experiment, 48 zebrafish larvae were placed in separate wells in two 24-well microtiter plates (Cat. No. 303002; Corning Costar, High Wycombe, UK) that were milled to a depth of 9 mm to reduce shadow and perspective artifacts. The output of the video recording system was typically as presented in Fig 1.

## III. POSE ESTIMATION

In this section, the procedure of estimating the poses of the zebrafish larvae from the input video files is described. First, the possible regions of movement of the larvae and a static background image are estimated. Then the poses of the larvae are estimated in each region using difference images created by subtracting the estimated background from the current frame.

### A. Calibration

Each zebrafish larva is placed in a well in one of the microtiter plates and is constrained to move within the bounds of the well. Consequently, the tracking problem can be formulated as the independent tracking of 48 larvae. Furthermore, the fact that the wells are identically shaped is used for subsequent analysis of zebrafish larvae behavior, where the center of each of the wells is used to define a local coordinate system for each larvae.

The positions of the wells are estimated as follows. First, geometrical models of the microtiter plates are created using the

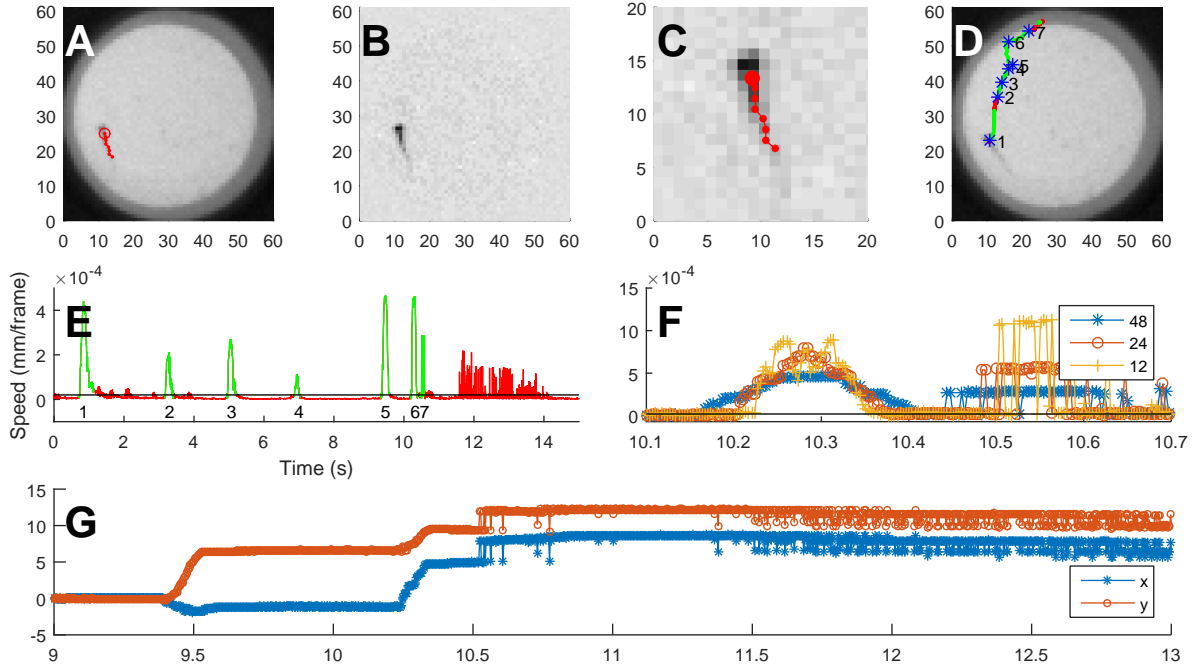


Fig. 2. Tracking and data. (A) shows a subsection of a video frame displaying the well of one larva, with the estimated larva pose superimposed in red. (B) shows the image in (A) after subtracting the background image. (C) shows a subsection of (B) with the larva pose superimposed in red. (D) shows the trajectory of the head position a larva superimposed on an image from the video. The trajectory is colored green at the points belonging to a swim bout, and red elsewhere. The blue asterisks represent the start of a swim bout numbered according to the number next to it. (E) shows the robustified speed function (see equation (3)) for the larva in blue and the threshold used for swim bout detection as the straight line in black. (F) shows the speed measure  $v_k(t)$  from Eq (4) at the time around swim bout number 7 for  $k = 12, 24, 48$ . (G) shows the tracked  $x$  and  $y$ -coordinates of the head independently for a section of the time. Note the oscillatory noise that is successfully classified as not being part of an actual movement.

known radii of the wells and the distances between them. Secondly, a thresholding procedure provides a number of circular blobs corresponding to the wells. Thirdly, affine transformations  $A_1$  and  $A_2$  from the models of the microtiter plates to the center of the blobs are estimated using RANSAC and linear least squares. Lastly, the regions that are subject to tracking is found by projecting the well-regions in the geometrical models of the microtiter plates. An example of calibration results is shown in Fig 1. Additionally, tracked pixel coordinates of larvae can be transformed to the units in the geometrical model (e.g. millimeters) by applying the inverse of the estimated transformations.

### B. Background estimation

The static background is estimated by first modeling each pixel  $(i, j)$  as belonging to one of two Gaussian distributions (with expected values  $F_{ij}$  and  $B_{ij}$ ) and subsequently estimating the distributions. The distributions are estimated in an iterative procedure defined as follows. Initialization is provided by computing the mean value  $M_{ij}$  of each pixel  $(i, j)$  over a set of randomly selected frames. The darker distributions are assigned the mean minus  $\epsilon$  and the brighter distributions are assigned the mean plus  $\epsilon$ , i.e.  $F_{ij}^{(0)} = M_{ij} - \epsilon$  and  $B_{ij}^{(0)} = M_{ij} + \epsilon$ , for some small  $\epsilon > 0$ . For a random image  $I$  and for each pixel, the distance from the brighter distribution to the image and from the darker distribution to the image is compared, and

the closest distribution is updated using moving average. After  $N = 1000$  iterations, the estimates have usually converged and the procedure is finished. Since the larvae are dark and the background is bright, the background is defined as the estimated brighter distribution.

### C. Pose-estimation

The pose of a zebrafish larva is estimated by first finding the head position and then tracing the tail by adding points that are incrementally more distant from the head. Each point is estimated in sub-pixel resolution by linear (the tail) or quadratic interpolation (the head).

For this purpose, a Gaussian smoothing is applied on the difference image  $F = I - B$  and the position of the maximal value provides an initial estimate of the head position in pixel-resolution. The use of the position of the maximum as the head position works sufficiently well due to the quality of the difference images (cf. Fig 2(B-C)) and the shape of the larva. The initial estimate is improved upon in the  $x$  and  $y$ -directions independently by fitting quadratic polynomials to  $5 \times 1$  and  $1 \times 5$  neighborhoods around the initial position estimate. The sub-pixel estimate of the head position  $(x_0, y_0)$  is defined as the position of maximal value of the fitted polynomials.

The tail of the larva is traced by finding the maximal values in a set of  $N_{points}$  circles of increasing radii centered at

$(x_0, y_0)$ , i.e.

$$(x_k, y_k) = \underset{(x,y) \in \Omega(x_0, y_0; r_k)}{\operatorname{argmax}} F(x, y), \quad k = 1, \dots, N_{\text{points}} - 1, \quad (1)$$

where  $F(x, y)$  is evaluated by linear interpolation of  $F$  using the four neighboring pixels of the point  $(x, y)$ ,  $\Omega(x_0, y_0; r_k)$  is the set containing all points on the circle of radius  $r_k$  centered at  $(x_0, y_0)$  and  $N_{\text{points}} - 1$  is the number of sought points on the tail.

Additionally, the foreground pixel intensities ( $q_k = F(x_k, y_k)$ ) at the estimated points are stored and used as a quality measure. This means that for each larva and frame, there are  $3N_{\text{points}}$  values stored:

$$(x_0, y_0, q_0, \dots, x_{N_{\text{points}}-1}, y_{N_{\text{points}}-1}, q_{N_{\text{points}}-1}). \quad (2)$$

The pose estimation procedure is repeated for each larva in every frame, creating data on the form  $(x_{i,j,k}, y_{i,j,k}, q_{i,j,k})$ , where  $i \in [0, N_{\text{points}} - 1]$  is the point index,  $j \in [1, N_{\text{frames}}]$  is the frame number and  $k \in [1, N_{\text{larvae}}]$  is the larva number.

#### IV. BEHAVIORAL ANALYSIS

The zebrafish larvae move in discrete movements referred to as *swim bouts*. This section describes how the swim bouts are detected and normalized and resampled to enable meaningful comparisons of different swim bouts. A clustering method is then applied on the data in order to create a set of cluster centers later used for classifying swim bouts. The classification results are used in Section V to analyze the behavior of the zebrafish larvae.

##### A. Swim bouts

A swim bout is defined as the time interval where the speed of the larva is greater than some threshold. Due to the presence of oscillatory tracking noise (see Fig 2(G)), a speed measure that is robust to such noise is necessary. For this purpose, the robustified speed measure  $\hat{v}(t)$  is defined as

$$\hat{v}(t) = \min_{k \in S} v_k(t), \quad (3)$$

where  $v_k(t)$  is the average speed over a time window of width  $k$  and centered at  $t$ , i.e.

$$v_k(t) = \frac{FPS}{k} \left\| \begin{bmatrix} x(t+k/2) - x(t-k/2) \\ y(t+k/2) - y(t-k/2) \end{bmatrix} \right\|_2 \quad (4)$$

where  $FPS$  is the frame rate ( $FPS = 300$  in this case). In this paper, the set of window sizes  $S = 12, 24, 48$  provides a qualitatively good compromise between detecting true swim bouts and rejecting false swim bouts. Visualizations of Eq (3) and Eq (4) on real data are presented in Fig 2(E) and Fig 2(F).

A potential swim bout interval is defined as the time interval where the estimated robustified speed  $\hat{v}(x, y, t)$  is larger than a threshold  $v_{thr} = 0.2 \cdot 10^{-4}$  mm/frame. An example of the activity function and threshold can be seen in Fig 2(E). This clearly supports the idea of treating the behavior of the zebrafish larvae as discrete swim bouts.

The potential swim bout intervals are post-processed by a combination of dilation, erosion and removing intervals that

have low likelihood values (the  $q$ -value that was introduced in Section III-C). This procedure has the effect that intervals that are close enough are merged and intervals that are too short or where the estimated tracking quality is too low are removed. Some potential swim bout intervals that are removed during post-processing can be seen in Fig 2(E).

##### B. Swim bout classification

In order to compare different swim bouts, a way of measuring distances between swim bouts with different numbers of frames is needed. To achieve this, the trajectory of the swim bouts were equidistantly (in space) subsampled with  $K$  samples and time was added as a dimension. Thus the trajectory of each swim bout was represented on the form

$$SB_i : X^{(i)} = \begin{bmatrix} x_1^{(i)} & x_2^{(i)} & \dots & x_K^{(i)} \\ y_1^{(i)} & y_2^{(i)} & \dots & y_K^{(i)} \\ t_1^{(i)} & t_2^{(i)} & \dots & t_K^{(i)} \end{bmatrix} \quad (5)$$

Thus data for all swim bouts can be represented by column stacking the resampled swim bouts in the matrix  $X = [X^{(1)} X^{(2)} \dots X^{(N_{\text{bouts}})}]$ .

As indicated by Fig 3(C), the space of swim bouts appears to be continuous without any apparent clusters. However, it is still meaningful to somehow bin the data. For this purpose, a clustering method (k-means is used in this paper) is applied to separate the data into groups. Before applying the k-means method on  $X$ , the data is normalized to remove the effect of the starting position and direction. Therefore, each swim bout is transformed by a rigid transformation with the effect that it starts in the origin and is headed to the right, as shown in Fig 3. The k-means method subsequently produces  $K = 15$  (defined empirically) groups that can be used for classification of swim bouts.

#### V. EXPERIMENTS AND RESULTS

The data set used in this paper contains three experiments on Amphetamine, two on Apomorphine and one control experiment.

Drug experiments were conducted on 10 days post fertilization (dpf) zebrafish larvae which were first placed in the wells and video recorded for 5 minutes, then drugs or placebo were injected in the wells followed by recording of videos for 50 or 60 minutes. In order to study the effects induced by various doses, the 48 larvae were split into 4 equally populated groups: a control group and low, medium and high dose groups.

Similarly, the control experiment was conducted on 10 dpf zebrafish larvae by recording for 60 minutes but without any interference in any subgroup of larvae.

A subset of the data is visualized in Fig 4 by plotting the distributions of swim bout classifications over time (bottom row) and on average (top row). The time-dependent plots are created by splitting up time into a number of non-overlapping intervals of length 150 seconds. The distribution of swim bout classifications is computed for all swim bouts in each such interval. To increase readability of the figure, a subset of 5 swim bout classes has been selected for plotting. Here, only the

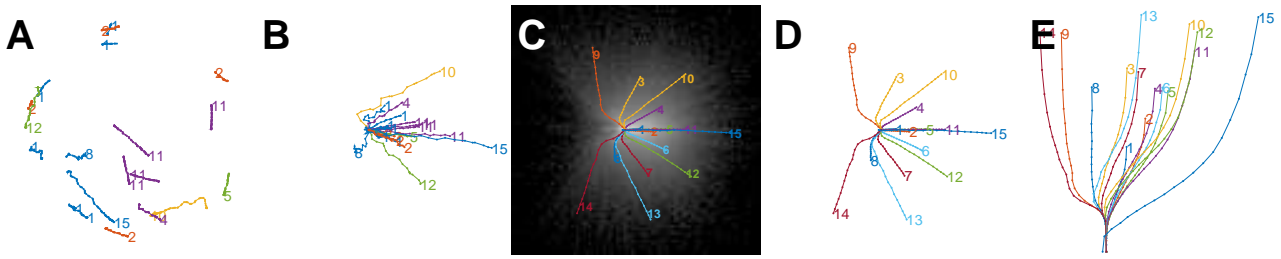


Fig. 3. Swim bouts and classification thereof. (A) shows the trajectories of 20 randomly selected swim bouts, with class numbers printed next to them. (B) shows the trajectories of the swim bouts from (A) after normalization and resampling (see Section IV-B). The element-wise logarithm of the density image of the full set of normalized and resampled trajectories is presented in (C), with the mean trajectories from (D) superimposed. (D) and (E) shows the  $(x, y)$  and  $(x, t)$  coordinates, respectively, of the mean trajectories (see Section IV-B). Note that the scale of (B), (C) and (D) are equal and the other scales are different.

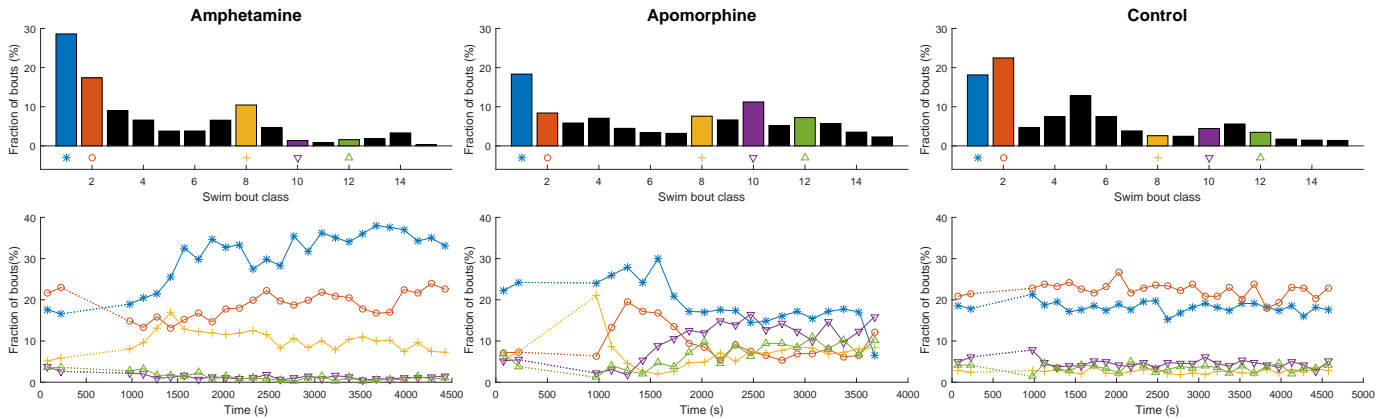


Fig. 4. Distribution of bout class observations. The top row shows the time-average distributions of bout classifications in each experiment (see Section V). In the bottom row, bout class distributions are plotted in 150s non-overlapping time bins. The bars in the top row that are visualized over time in the bottom row have different colors, while the rest of the bars are black. In addition, the selected classes have a marker below their respective bars that is the same as in the time-dependent plot. The dotted lines denote the time during which drugs are induced. Note that the classes and their numbers are the same as in Fig 3, but the colors are in general not the same.

data generated by the 48 larvae in the control experiment, the 36 larvae given the highest dose ( $10\mu M$ ) of Amphetamine, and the 24 larvae given the highest dose ( $50\mu M$ ) of Apomorphine, is presented.

## VI. DISCUSSION

The preliminary data presented in Fig 4 clearly shows that the proposed method is able to show the difference in behavior induced by Apomorphine and Amphetamine in the zebrafish larvae. For example, the Amphetamine-treated larvae tends to increasingly favor shorter movements (class 1). Furthermore, it is shown that there is a time-dependency in the induced drug effects, for example the sharp rightwards turn (class 8) is not very common in the pre-drug control time interval but is observed a lot more for a period directly after inducing Apomorphine.

## REFERENCES

- [1] J. Cachat, A. Stewart, E. Utterback, P. Hart, S. Gaikwad, K. Wong, E. Kyzar, N. Wu, and A. V. Kalueff, "Three-dimensional neurophenotyping of adult zebrafish behavior," *PLoS one*, vol. 6, no. 3, p. e17597, 2011.
- [2] C. E. Vargas-Irwin, G. Shakhnarovich, P. Yadollahpour, J. M. Mislow, M. J. Black, and J. P. Donoghue, "Decoding complete reach and grasp actions from local primary motor cortex populations," *The Journal of Neuroscience*, vol. 30, no. 29, pp. 9659–9669, 2010.
- [3] T. Palmér, M. Tamtè, P. Halje, O. Enqvist, and P. Petersson, "A system for automated tracking of motor components in neurophysiological research," *Journal of neuroscience methods*, vol. 205, no. 2, pp. 334–344, 2012.
- [4] M. Santana, T. Palmér, H. Simplicio, R. Fuentes, and P. Petersson, "Characterization of long-term motor deficits in the 6-ohda model of parkinson's disease in the common marmoset," *Behavioural brain research*, vol. 290, pp. 90–101, 2015.
- [5] J. Tian, A. Satpathy, E. S. Ng, S. G. Ong, W. Cheng, J.-M. Burgunder, and W. Hunziker, "Motion analytics of zebrafish using fine motor kinematics and multi-view trajectory," *Multimedia Systems*, pp. 1–11, 2014.
- [6] G. Bianco, V. Botte, L. Dubroca, M. R. dAlcalà, and M. G. Mazzocchi, "Unexpected regularity in swimming behavior of clausocalanus furcatus revealed by a telecentric 3d computer vision system," *PLoS one*, vol. 8, no. 6, p. e67640, 2013.
- [7] M. T. Ekvall, G. Bianco, S. Linse, H. Linke, J. Bäckman, and L.-A. Hansson, "Three-dimensional tracking of small aquatic organisms using fluorescent nanoparticles," *PLoS one*, vol. 8, no. 11, p. e78498, 2013.
- [8] T. Pinkiewicz, G. Purser, and R. Williams, "A computer vision system to analyse the swimming behaviour of farmed fish in commercial aquaculture facilities: a case study using cage-held atlantic salmon," *Aquacultural Engineering*, vol. 45, no. 1, pp. 20–27, 2011.
- [9] C. Spampinato, S. Palazzo, D. Giordano, I. Kavasidis, F.-P. Lin, and Y.-T. Lin, "Covariance based fish tracking in real-life underwater environment," in *VISAPP (2)*, 2012, pp. 409–414.
- [10] C. Beyan and R. B. Fisher, "Detection of abnormal fish trajectories using a clustering based hierarchical classifier," in *BMVC*, 2013.
- [11] E. Fontaine, D. Lentink, S. Kranenbarg, U. K. Müller, J. L. van Leeuwen, A. H. Barr, and J. W. Burdick, "Automated visual tracking for studying the ontogeny of zebrafish swimming," *Journal of Experimental Biology*, vol. 211, no. 8, pp. 1305–1316, 2008.